Physicochemical properties of Aquivion/fluorine grafted sepiolite electrolyte membranes for use in PEMFC

Sahng Hyuck Woo, Aurelie Taguet, Belkacem Otazaghine, Annette Mosdale, Arnaud Rigacci, Christian Beauger

Physicochemical properties of Aquivion/fluorine grafted sepiolite electrolyte membranes for use in PEMFC

Sahng Hyuck Woo [a], Aurélie Taguet [b], Belkacem Otazaghine [b], Annette Mosdale [c], Arnaud Rigacci [a], Christian Beauger [a, *]

[a] MINES ParisTech, PSL University, Center for Processes, Renewable Energy and Energy Systems (PERSEE), CS 10207 rue Claude Daunesse, F-06904, Sophia Antipolis Cedex, France
[b] Centre des Matériaux des Mines d'Alès (C2MA), IMT – Mines Alès, 6 Avenue de Clavières, F-30319, Alès Cedex, France
[c] Symbio, 14 rue Jean-Pierre Timbaud, Espace des Vouillands 2, 38600 Fontaine, France

A B S T R A C T

This study proposes a novel sepiolite-based Aquivion electrolyte membrane which could be operated at low relative humidity. In the study, it was discovered that the functionalization of sepiolite with fluorinated groups (i.e., $-C_7F_{15}$), named SEP-F, helps its dispersion in the composite membrane, compared with the use of natural sepiolite. The Aquivion/SEP-F composite membrane showed increased water uptake, thermo-mechanical and chemical stability as well as proton conductivity and decreased swelling compared with commercially available Nafion HP and pristine Aquivion. Their behavior in single cell MEA testing conditions was also assessed. Aquivion/SEP-F composite membrane can be an interesting alternative for low relative humidity operation of PEMFC (proton exchange membrane fuel cell).

Keywords:
Aquivion
Perfluorosulfonic acid (PFSA)
Sepiolite nanofiber
Fluorination
Proton exchange membrane fuel cell (PEMFC)

1. Introduction

Fuel cells are effective devices to mitigate carbon dioxide emissions from combustion, using hydrogen as an energy source. Hence fuel cells are potentially eco-friendly energy converters with a positive impact on climate change. A description of the various fuel cells is set forth in Refs. [1,2]. In particular, PEMFCs have been used in automobile applications due to their advantages such as portable power, low operating temperature, high efficiency, harmless electrolytes and high power density.

Among the broad range of polymers used in proton exchange membranes (PEMs), Nafion, one of PFSA materials, has been widely adopted as standard because of its rather good thermal and chemical stability, mechanical strength, hydrophilicity and MEA (membrane electrode assembly) performance at low temperature, resulting from both its chemical composition and chain organization: PTFE-like backbones and polyethers having side chains terminated with sulfonic acid groups ($-SO_3H$) [3,4]. However, physicochemical characteristics of pristine Nafion membrane are limiting the PEMFC operation range. The proton conductivity of the electrolyte membrane declines due to dehydration as PEMFCs are operated at intermediate temperature, that is above 100°C. In addition, among PFSA materials, Aquivion has been selected for its enhanced proton conductivity and thermal stability compared with those of Nafion due to short-side-chain, larger crystallinity, higher glass transition temperature, and lower equivalent weight [5,6]. Aquivion membranes are also chemically stable and can operate at temperatures higher than Nafion membrane. According to result of Aricò's group, Nafion membrane has a maximum operating temperature of 95°C, while Aquivion membrane can be operated up to 110°C [7]. Higher PEMFC operating temperature can lead to carbon monoxide (CO) tolerance, easier heat and water management and better reaction kinetics during operation [8,9].

Various inorganic fillers have been used as additives to develop composite membranes suitable for use at low relative humidity. The incorporation of such fillers results in increased water uptake and sometimes proton conductivity and mechanical resistance.

* Corresponding author.
E-mail addresses: sahngh.woo@gmail.com (S.H. Woo), aurelie.taguet@mines-ales.fr (A. Taguet), belkacem.otazaghine@mines-ales.fr (B. Otazaghine), annette.mosdale@symbio.one (A. Mosdale), arnaud.rigacci@mines-paristech.fr (A. Rigacci), christian.beauger@mines-paristech.fr (C. Beauger).

Inorganic fillers added in composite membranes include inorganic oxides, e.g., TiO_2, SiO_2, ZrO_2, and ZrO_2/SO_4^{2-} [10–20]; and zeolites, e.g., NaA zeolite, ETS-10, umbite, mordenite, analcime, faujasite, b-zeolite, ZrP-modified zeolite, and H-type of b-zeolite [10,21–25], and nanoclays, e.g., montmorillonite, laponite, sepiolite or halloysite [10,21,26–33].

Incorporation of nanoclays into a polymer matrix helps to overcome some of the limitations regarding thermo-mechanical resistance and sensitivity to relative humidity at high temperature. Blending of nanoclay particularly prevents dehydration due to its hydroscopic property. Composite membranes can be in turn operated at low relative humidity [30,34–38]. Mechanical properties may also be improved through fillers homogeneous dispersion, functionalization for better compatibility with the polymer selected for the composite membrane or exfoliation in case of some nanoclays [36,38–41]. The presence of fillers can, moreover, decrease the hydrogen crossover [42,43]. Also, according to literature published by Peighambardoust, S. Jamai et al., nanoclay-based membranes are cost competitive compared with inorganic oxide materials and zeolites-based composite membrane [10,44]. In particular, sepiolite (SEP), a natural nanoclay, has a fibrous morphology (so called needle-like structure) and consists of parallel tunnels formed by blocks. Hence, it is able to improve the tensile strength of the membrane by the effect of chain packing [35,36,39,45,46]. The authors already demonstrated in previous studies that the incorporation of sepiolite can lead to improved mechanical properties of Nafion composite membranes [35,36]. However, aggregated nanoclays inside the polymer matrix can hinder the expected benefit. Hence, controlling the dispersion state of sepiolite has been considered as a crucial challenge in order to enhance the performance. To this end, surface modification of sepiolite has been achieved, namely sulfonation [29,36,47] or perfluorosulfonation [35]. The nanoclay dispersion process also proved to be an important step [48].

It is noteworthy that PFSA membranes are chemically degraded by free radical species which can be formed during fuel cell operation, i.e., HO· and HO_2· with strong oxidative property. Such free radicals chemically attack C-F bonds thus impacting the permeability of the membrane resulting in an increase of H_2 crossover [49]. The formation of H_2O_2 can be generated at the cathode side of the MEA following a two-electron reduction reaction of oxygen. H_2O_2 can then react with divalent iron (Fe^{2+}) to form free radical species such as HO· and HO_2· [10,50–52]. The free radical formation pathway at the cathode can be described by the following equations [10,50]:

1) $O_2 + 2H^+ + 2e^- \rightarrow H_2O_2$
2) $H_2O_2 + Fe^{2+} \rightarrow Fe^{3+} + HO\cdot + HO^-$
3) $HO\cdot + H_2O_2 \rightarrow H_2O + HO_2\cdot$

To date, the influence of the incorporation of sepiolite in short-side-chain PFSA membranes has not been fully investigated for PEMFC application even though Aquivion is a prominent candidate as one of PFSA ionomers. Moreover, the impact of sepiolite modification on Aquivion membrane features has not been fully demonstrated. If so, modified sepiolite-based Aquivion composite membranes may enhance fuel cell performance under extended range of PEMFCs operating conditions.

The present study proposes a novel sepiolite-based Aquivion composite membrane which can be operated in low relative humidity. In this study, the authors evidenced that fluorinated sepiolite improved the properties of Aquivion composite membrane, compared with pristine sepiolite-based composite membranes. The membrane actually displayed superior water uptake and proton conductivity compared with commercially available membranes such as Nafion HP membranes, selected as the reference, on top of increased mechanical properties compared with pristine Aquivion membrane. Chemical stability against radical attack was, moreover, demonstrated. Finally, the performance in a fuel cell single cell was assessed at different conditions of relative humidity.

2. Experimental

2.1. Materials

Sepiolite was provided by Tolsa. Pangel S9 sepiolite used as additive in this study consists of 85% of sepiolite and 15% of other clays. N-(3-triethoxysilylpropyl)perfluorooctanoamide (SPFOA) was purchased from ABCR. Ethanol, acetone and tetrahydrofuran (THF) were purchased from Fisher Chemical. All these products were used for functionalization without further purification.

Aquivion (24%, D83-24B) was purchased from Solvay. Sulfuric acid (H_2SO_4, 5 N), sodium hydroxide (NaOH, 98%) and hydrogen chloride (HCl, 0.1 N) were purchased from Alfa Aesar, Germany. Hydrogen peroxide (H_2O_2, 30%) was purchased from Fisher Scientific, UK. Sodium chloride (NaCl, 99.5%) and isopropanol (99.5%) were purchased from Acros Organics. Total ionic strength adjustment buffer solution (TISAB IV) and sodium fluoride (NaF) were purchased from Sigma Aldrich. Deionized (DI) water (18.2 MΩ cm) was supplied from ultrapure water plants (Smart2Pure, Thermo Scientific).

2.2. Experimental methods

2.2.1. Sepiolite modification (see Scheme 1)

Into a 250 ml flask fitted with a condenser were introduced 10 g of sepiolite, 1 g (1.6×10^{-3} mol) of SPFOA and 100 ml of an ethanol/water (90/10 wt%) solution. The mixture was then stirred and heated at solvent reflux for 15 h. The mixture was next centrifuged (5000 rpm) to eliminate the liquid phase and washed twice with

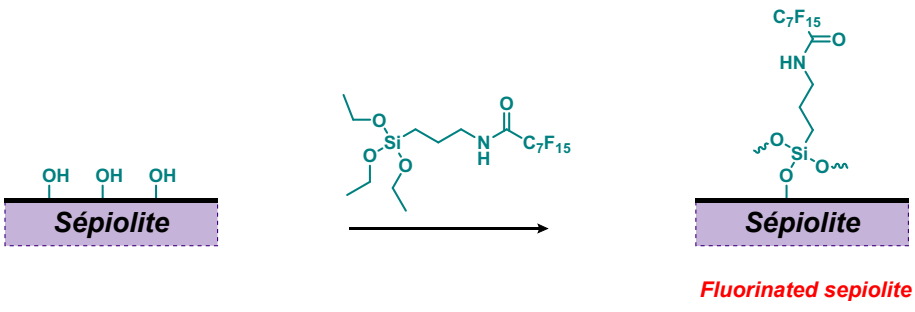

Scheme 1. Schematic representation of sepiolite nanofiber perfluorination grafted with N-(3-triethoxysilylpropyl)-perfluorooctanoamide (SPFOA).

acetone and THF. Finally, the modified filler was dried under vacuum before characterization.

All sepiolite materials (pristine or modified) were filtered using different membrane filters (45 μm and 25 μm pore sizes, Merck Millipore) and then dehydrated in oven at 80°*C* for 16 h.

In terms of nomenclature, pristine sepiolite and fluorinated sepiolite are labeled SEP and SEP-F, respectively.

2.2.2. Membrane preparation

Membranes with a size of 13 × 13 cm^2 were prepared via casting and evaporation. Commercially available Aquivion D83-24B ionomer dispersion (24%) provided by Solvay, sepiolite (pristine or modified) and isopropanol were blended in order to obtain a 5% Aquivion casting dispersion. Aquivion PFSA dispersions are based on the short side chain copolymer of tetrafluoroethylene (TFE) and sulfonyl fluoride vinyl ether (SFVE) produced by Solvay.

Casting dispersions were stirred for 15 min at 80 rpm prior to an ultrasound treatment (HD 2200, Bandelin, Germany) for 2 min at 60 W and 20% pulsation level. The resultant dispersions were poured in a mold, after which it was heated in oven at 80°*C* for 18 h and then at 170°*C* for 2 h. After evaporation 10 wt% sepiolite-loaded composite membranes were obtained. Prepared membranes were treated using 0.5 M H_2SO_4 for 1 h and washed with DI-water for 1 h at 100°*C*. Commercially available Nafion HP membrane was also treated the same way before characterization.

2.3. Analytical methods

2.3.1. ATR-FTIR

Fourier transform infrared (FTIR) spectroscopy was used to characterize the surface modification of sepiolite. Analyses were carried out using a spectrometer IFS 66 from Bruker. Each spectrum (400 and 4000 cm^{-1}) was obtained by collecting 32 scans with a resolution of 4 cm^{-1}.

2.3.2. TGA

The thermal stability of the sepiolite samples was studied by thermal gravimetric analysis (TGA). The analyses were performed by a thermogravimetric analyzer (Perkin Elmer Pyris-1 instrument). In order to remove all the physisorbed water, an isothermal step (10 min, 110 °C) was performed before starting the analysis and then the samples were heated to 900 °C at a heating rate of 10 °C/min. Measurements were carried out under nitrogen atmosphere with a flow rate of 20 ml/min on samples of approximately 10 mg.

2.3.3. Py-GC/MS

Samples were pyrolyzed using a Pyroprobe 5000 pyrolyzer (CDS Analytical). Each sample (<1 mg) was placed in a quartz tube between two pieces of rockwool and was then heated at 900 °C with an electrically heated platinum filament. The sample was heated for 15 s and gases formed by thermal decomposition were drawn to a 450-GC chromatograph from Varian with a split ratio set to 1:50. For the GC analysis, the temperature was raised from 70 °C to 310 °C at 10 °C/min. Helium (1 l/min) was chosen as gas carrier combined with a Vf-5 ms capillary column (30 m × 0.25 mm; thickness = 0.25 μm). After separation, the gases were analyzed using a 240-MS mass spectrometer from Varian.

2.3.4. FE-SEM and EDS

The cross section of prepared membranes was examined using FE-SEM (Field emission scanning electron microscopy, FEI XL30, Philips) at 2000× magnification. Si/F atomic ratio (%) across the membrane cross section was calculated using EDS (Energy dispersive X-ray spectroscopy), in order to confirm sepiolite distribution inside the polymer matrix.

2.3.5. Membrane thickness

Wet membranes were cut into seven pieces and the thickness of three pieces selected diagonaly was measured on three different locations using a micrometer (Mitutoyo 293−344, Japan). The average thickness of each membrane could then be calculated based on the nine measurements data. The thickness of the dried membranes was also measured on cross-sections using FE-SEM. (six measurements per each membrane were averaged).

2.3.6. Water uptake

The water uptake was measured by weight difference between wet and dried membranes. The membranes were first immersed in DI water at room temperature and their weight measured after wiping the excess of water (W_w). The weight of the dried membranes (W_d) was then measured after drying in an oven at 80°*C* for 18 h. The water uptake was finally calculated according to the following equation:

$$W_{ut}\ (\%) = \frac{W_w - W_d}{W_d} \times 100 \tag{1}$$

where W_w and W_d are the weight of the wet and dried membranes, respectively.

2.3.7. Swelling ratio

Two kinds of swelling were calculated as the percentage of thickness difference between i. dry and wet membranes at room temperature and ii. wet membranes immersed 2 h in water at room and boiling temperature. The thickness was measured as mentioned in 2.3.5 and the swelling was calculated based on the following equations:

$$S_{th\_1}(\%) = \frac{th_{wet\_rt} - th_{dry}}{th_{dry}} \times 100 \tag{2}$$

$$S_{th\_2}(\%) = \frac{th_{wet\_bt} - th_{wet\_rt}}{th_{bt\ wet\_rt}} \times 100 \tag{3}$$

where th_{dry} th_{wet_rt} and th_{wet_bt} are the thickness of the dry membranes and membranes immersed in water at room temperature and 100°*C*, respectively.

2.3.8. IEC (ion exchange capacity)

IEC was measured by titration. The membranes were fully immersed for 24 h in 40 ml of 2 N NaCl solution for Na^+ ions to replace H^+ ones in the membrane. H^+ ions were then titrated with 0.005 N NaOH solution. IEC was calculated according to the following equation:

$$IEC\ (meq/g) = \frac{V_{NaOH} \times C_{NaOH}}{W_d} \tag{4}$$

where V_{NaOH} and C_{NaOH} are the volume and the concentration of NaOH, respectively. W_d is the weight of dried membranes.

2.3.9. Chemical stability

Chemical degradation of the membrane may occur due to the presence of iron through C-F bond attack during fuel cell operation. Such a process results in an increase in the fluorine concentration in the water produced by the fuel cell. The chemical stability can thus be assessed through the analysis of the fluorine concentration.

Since iron may be present in Sepiolite and contribute to the degradation of the membrane, a modified Fenton test was applied, immersing the membranes in a 4.4 M H_2O_2/1.25 mM H_2SO_4 solution, the sepiolite being considered as the source of iron. One piece

of wet membrane was immersed for 4 h, 17 h, 48 h, 72 h and 96 h in a brown glass bottle containing the afore-mentioned solution in order to reach 0.16 wt%. The solution temperature and stirrer speed were set at 80°*C* and 100 rpm, respectively. The fluoride concentration in the solution added with TISAB IV was then analyzed using an ion meter and a specific electrode (781 pH/Ion meter, Metrohm AG, Swizerland). 0.001 N NaF aliquotes were added as a standard during analysis. A blank test of the solution was conducted prior to any analysis.

The iron content of sepiolite nanoparticles was analyzed using EDS during SEM observation.

2.3.10. DMA (dynamic mechanical analysis)

The viscoelastic behavior of the membranes was determined using dynamic mechanical analysis (DMA50 from Metravib, Acoem) under shear jaws for film test configuration. The samples dimension was 30 mm length, 10 mm height and the thickness of the membrane (between 30 and 50 μm). The results were analyzed with DYNATEST software. A temperature scan was performed on membranes from 50 to 200 °C at a heating rate of 1 °C/min. It was verified previously that the deformation (3 μm) was in the linear domain. The frequency was 1Hz. Since membranes are very thin (around 40 μm in wet state) the reproducibility is not high but still some trends can be observed.

2.3.11. EIS (electrochemical impedance spectroscopy)

The through-plane resistance of membranes was accurately measured by electrochemical impedance spectroscopy (EIS, Bio-Logic Scientific Instruments HCP-803, France). The membrane sample was placed between two electrodes in a homemade cell for measurement under different conditions of temperature (50 °C, 70 °C, or 90 °C) and relative humidity (RH = 25%, 50%, 75%, or 90%). EIS equipment was operated under frequency range between 1 mHz and 1 kHz with an amplitude of ±20 mV. All resistance values (Ohm) of membranes were calculated by averaging high frequency values of the impedance for which the imaginary part equals zero. The proton conductivity (S cm^{-1}) of membranes was then calculated with the following equation:

$$\sigma = \left(\frac{1}{R}\right)\left(\frac{l}{S}\right) \quad (5)$$

where σ represents the proton conductivity (S cm^{-1}), R and l are resistance (ohm) and thickness (cm) of membrane, respectively. S represents the contact surface with electrodes (cm^2).

2.3.12. MEA preparation

Catalyst Coated Membranes were made with a SonoTek ExactaCoat ultrasonic spray-coating machine. The ExactaCoat coating machine is a programmable 3-axis robot with an integrated Accumist ultrasonic atomizing nozzle. The system is easily configured to customize spray patterns and to deposit precise amounts of ink. A syringe pump was used to supply the catalyst ink to the ultrasonic atomizing nozzle. The flow rate of the

catalyst ink delivery is controlled by the program software. The amount of ink deposited on the membrane, and hence the Pt loading of the CCM, is controlled by the ink flow rate and the x-y speed of the nozzle. The membranes were held down on a vacuum plate heated to 80 °C.

The catalyst used to prepare the ink for both the anode and cathode sides of the CCMs was Tanaka

TEC10E40E. The anode and cathode catalyst loadings were programmed for 0.3 and 0.5 mg Pt/cm^2 respectively.

Mass measurements made before and after coating confirmed the Pt loadings to be 0.26 ± 0.08 mg Pt/cm^2 for the anode and 0.50 ± 0.06 mg Pt/cm^2 for the cathode. 5L + SG MEAs (5-layer MEA + subgasket) were prepared by hot-pressing the gas diffusion layers (Freudenberg H23C6) and the PET subgaskets onto both sides of the CCMs at 170 °C and 50 kg/cm^2 for the Aquivion based membranes and 140 °C and 50 kg/cm^2 for the Nafion HP membrane. The anode and cathode GDLs were the same. Hot-pressing was carried out using a Carver 30-12H Press.

2.3.13. Single cell set-up and test protocols

The 5L + SG MEAs were set up in a 25 cm^2 single cell with graphite monopolar plates with a single channel flow field and with an integrated O-ring gasket. The cell was tightened with 8 nuts and bolts with a dynamometric wrench set at 6 Nm.

Fuel cell electrochemical tests were carried out with a BioLogic FCT-150S fuel cell test station. H_2 crossover tests were carried out with a BioLogic VSP potentiostat and a BioLogic VMP3 Booster.

Each MEA was activated at 0.6 V for 2–3 h until stabilization of the current.

Polarization curves (IV) were conducted at 80 °C in the co-flow configuration using pure hydrogen on the anode (stoichiometry = 1.5, outlet pressure = 2.5 bara, relative humidity = 30%) and air on the cathode (stoichiometry = 2.0, outlet pressure = 2.5 bara, relative humidity = 100% in wet mode and 30% in dry conditions). A more severe condition was also applied: low pressure = dry conditions + outlet pressure = 1.5 bara on both sides.

For resistance measurements, impedance spectroscopy (EIS) was carried out in the galvanostatic mode. An AC sinus signal (10% I amplitude) was applied around a fixed current I of 1.25 A, 20 A and 30 A (frequency range = [10 kHz–10 Hz]).

The hydrogen crossover was calculated after linear sweep voltammetry results obtained under H_2/N_2 at 3/3 bara. The voltage was scanned from 0.05 V to 0.55 V at 5 mV/s. The extrapolation of the straight linear portion between 0.4 and 0.5 V vs. RHE of the anodic current to zero cell voltage corresponds to the addition of the charging current and the current due to the oxidation of hydrogen crossed over from anode to cathode. The shorting resistance is the calculation of the ratio (slope) ($\Delta v/\Delta I$, [$\Omega.cm^2$]) between 0,4 V and 0,5 V vs. RHE.

To assess the durability of the membranes a highly accelerated stress test (HAST) from General Motor protocol was also conducted (dry conditions + cell temperature = 90 °C and outlet pressure = 3 bara): 1. Current Scan from 1,25 A–20 A in 10 s (1875 mA/s), 2. Current Scan from 20 A to 30 A in 60 s (167 mA/s), 3. 30 A for 35 s and 4. Current Pulse at 1.25 A for 160 s. The durability test is comprised of blocks of 5 h of HAST cycles (265 s) followed by shorting/crossover measurements, chronoamperometry, GEIS and IV tests. The AST test is stopped when the voltage reaches a value of 0.7 V at 0.05 A/cm^2 (or at OCV).

3. Results and discussion

3.1. Nanoclay characterization

Fluorinated and pristine sepiolite have been analyzed by FTIR spectroscopy (see Fig. 1). They show similar spectra with few differences. As already described for sepiolite samples, both spectra show O-H stretching vibrations from Mg_3OH in the 3600 cm^{-1} region [36]. The bands which appear at 978, 1008 and 1214 cm^{-1} were attributed to Si–O bonds within silica tetrahedra. Moreover a band around 1670 cm^{-1} was attributed to water molecules hydrogen bonded to the surface. Finally the bands appearing at 788, 685 and 646 cm^{-1} were also attributed to O-H vibrations from Mg_3OH (deformation at 788 cm^{-1} and bending at 685 and 646 cm^{-1}). For functionalized sepiolite, the FTIR spectrum shows

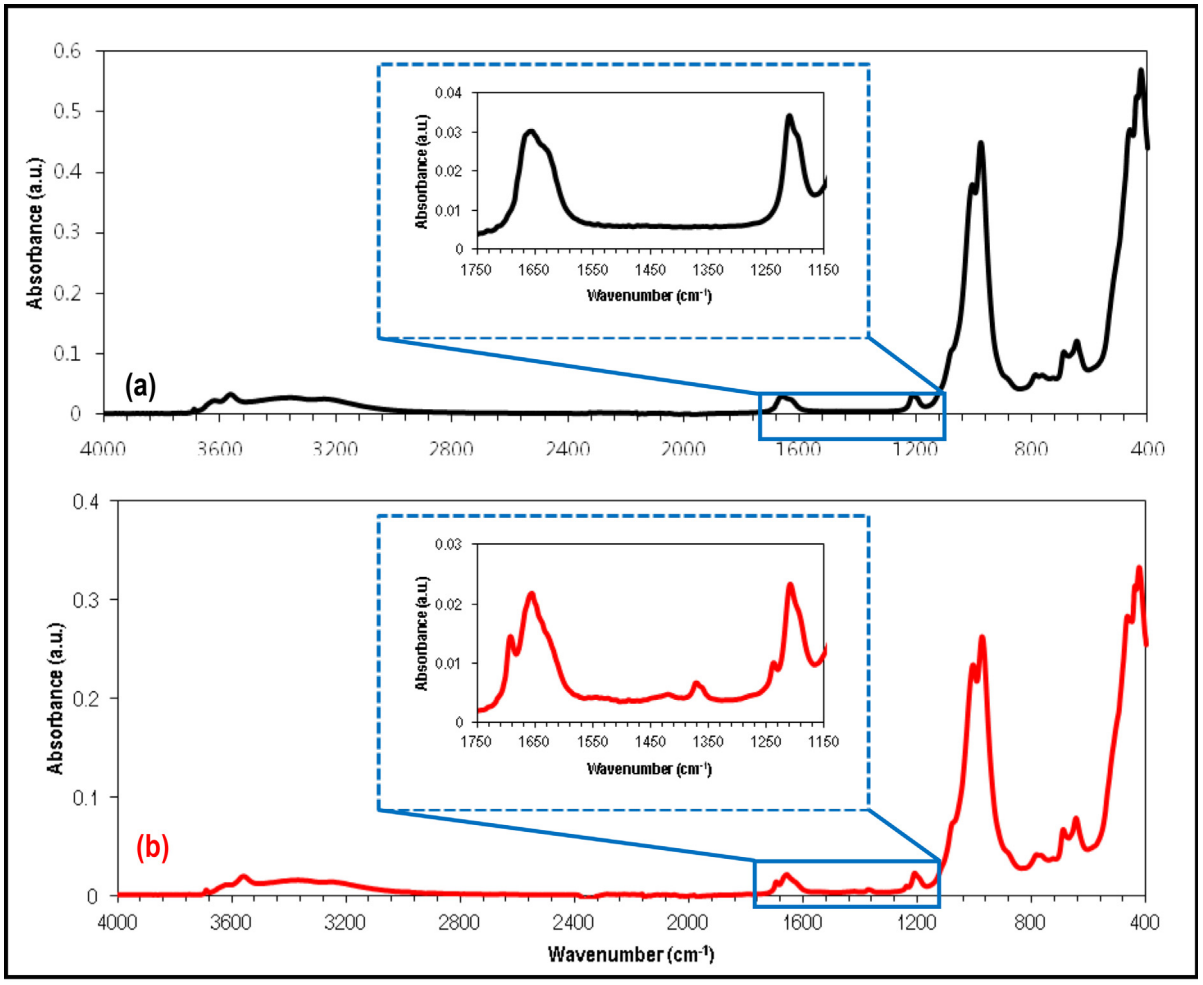

Fig. 1. ATR-FTIR spectra of (a) pristine sepiolite and (b) functionalized sepiolite.

some additional absorption peaks around 1240, 1370, 1420 and 1690 cm^{-1} attributed to the grafted organic part. Indeed, the band at 1240 cm^{-1} was attributed to the C-F bonds of the perfluorinated fragment. The bands at 1370 and 1420 cm^{-1} were attributed to C-H stretching vibrations of the alkyl part of the grafting agent. And finally the band at 1240 cm^{-1} was attributed to C═O stretching vibration of the amide function. The presence of these new bands proves the presence of the grafting agent for modified sepiolite after the functionalization procedure. Moreover, the shape of the band around 1670 cm^{-1} changes after the sepiolite treatment. Thermogravimetric analyses were used to characterize the functionalization of the sepiolite surface as shown in Fig. 2. The modified filler showed an increased weight loss after grafting of about 1.4%. This weight loss was attributed to the decomposition of the grafted organic part which tends to prove, along with FTIR results, the efficiency of the functionalization procedure used. If we take $Si_{12}Mg_8O_{30}(OH)_4(H2O)_4{,}8H_2O$ as the formula of sepiolite and assume that the weight loss (1.4 wt%) observed by TGA corresponds to the total degradation of the grafted organic part ($C_{11}H_7F_{15}NO$) then we can calculate a number of 4×10^{-2} alkyl chain grafted per unit formula of sepiolite.

Py–GC/MS was also used to validate the procedure of functionalization of sepiolite nanofibers. The analysis used a pyrolysis step at 900 °C to evaluate the presence and the nature of the organic molecules on the fillers surface. The results obtained for modified sepiolite additive (see Fig. 3) confirmed the TGA results.

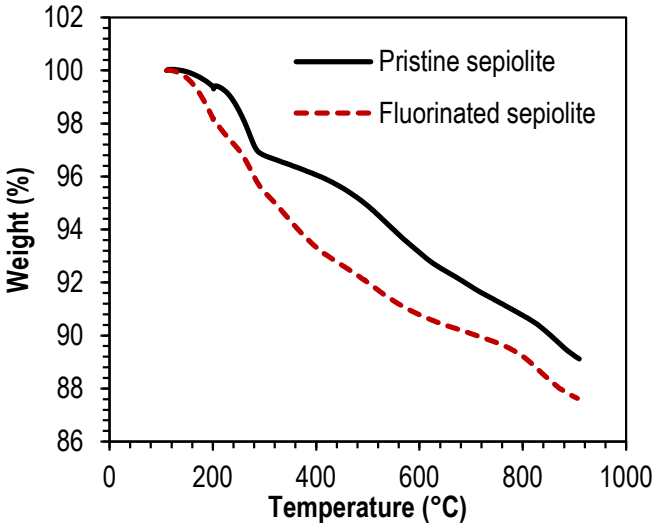

Fig. 2. TGA under nitrogen of pristine sepiolite and fluorine grafted sepiolite from 110 °C to 900 °C after an isotherm at 110 °C for 10 min.

Whereas no peak was observed for pristine sepiolite, the chromatogram of the functionalized clay shows peaks corresponding to organic molecules obtained by thermal degradation of the grafted

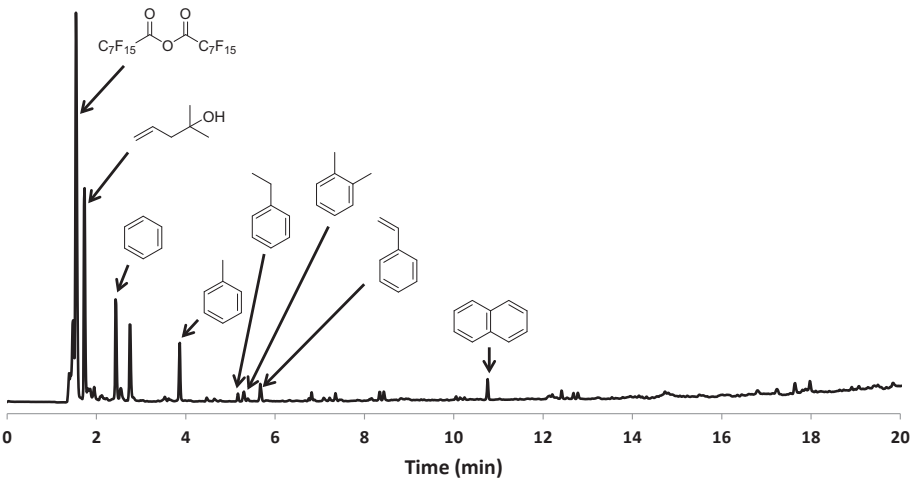

Fig. 3. Py–GC/MS chromatograms obtained for the modified sepiolite sample pyrolyzed at 900 °C.

part. Presence of fluorinated molecules is observed due to the perfluorinated group of the grafting agent. Different molecules like aromatic molecules are also observed. Their structure, which is far from that of the grafting agent, is due to fracture/recombination processes occurring during the thermal decomposition. So Py-GC/MS analysis confirmed the presence of the fluorinated grafting agent on the modified sepiolite nanofibers.

3.2. Membrane characterization

3.2.1. Thickness of hydrated membranes

The thickness of the membranes is an important feature for PEMFC application as thin membrane can lead to reduced resistance under the same condition [51], often at the expense of a higher hydrogen crossover. Hence, the membranes were prepared targeting a thickness of approximately 20 μm under dry conditions, similar to that of state-of-the-art commercial membrane Nafion HP.

The thickness of the dried Nafion HP, pristine Aquivion, Aq/sepiolite and Aq/fluorinated sepiolite membranes are close to the expected values: 22.7 ± 0.5, 24.6 ± 0.7, 25.6 ± 0.7 and 24.4 ± 0.4 μm, respectively. Few differences were observed between all the studied membranes. Note that for Nafion HP the thickness could also be mesasured using the micrometer since it was provided in a dry state. No significant difference was obtained compared to that measured on the SEM image (22.0 ± 0.9 μm versus 22.7 ± 0.5 μm).

Since the prepared membranes were recovered by dipping, in DI-water, the glass plate they are prepared on, their thickness was thus first measured in a wet state at room temperature. For comparison, the thickness of Nafion HP was measured in the same conditions. Data are gathered in Fig. 4a. The aquivion membrane prepared for the study came out to be significantly thicker than the Nafion HP one (32 μm vs 23 μm). Adding 10 wt% of sepiolite, pristine or grafted, resulted in an even much more increase of the membrane thickness up to 55 μm for both composites. Such difference will be considered when discussing the MEA fuel cell performances.

3.2.2. Ion exchange capacity

IEC is a representative indicator of the available number of ion exchange groups. It strongly influences the proton transfer through PEM, in particular Grotthuss-type transfer [53]. The IEC of the composite membranes showed similar values compared to that of pristine Aquivion and reference membranes as shown in Fig. 4b. Hence, the incorporation of sepiolite-type fillers, regardless of functionalization, does not impact the IEC. More specifically, the IEC of pristine Aquivion membrane displayed approximately 1.02 meq/g, whereas sepiolite-loaded composite membranes displayed values between 0.96 and 1.20 meq/g. Nafion HP membrane also exhibited similar IEC (1.08 meq/g) to pristine Aquivion membrane.

3.2.3. Water uptake

Water molecules are essential during proton transfer in ionomeric polymer matrix for hopping, named Grotthuss mechanism, or for vehicle mechanisms. The former means that protons randomly hop between neighbored protonic species such as H^+ and H_3O^+ through hydrogen-network, whereas the latter implies that protons are diffused together with water molecules by forming hydronium ions, e.g., H_3O^+, $H_5O_2^+$, and $H_9O_4^+$, caused by electrochemical difference [46,54,55]. Hence, the water uptake of the membranes impacts the proton transfer during PEMFC operation.

As shown in Fig. 4c, the water uptake of our prepared Aquivion membrane and that of Nafion HP are rather similar (30–38%). The introduction of sepiolite in Aquivion is highly beneficial since it resulted in almost doubling water uptake, reaching around 70%. This can be attributed to the hydroscopic property of the numerous silanol groups (Si-OH) available in sepiolite. It is noteworthy that the functionalization of sepiolite did not affect the water uptake very much, even with less silanols and the introduction of hydrophobic fluorinated groups.

3.2.4. Swelling ratio

Swelling is another important feature since too high a value can impact fuel cell performance during operation.

The swelling calculated between dry and wet states of membranes at room temperature (Eq. (2)) showed significant differences between the prepared membranes (Fig. 4d). First of all the prepared Aquivion membrane showed a much higher swelling than the commercial Nafion HP, 31% versus 2%. This is consistent with the fact that Nafion HP is reinforced whereas the prepared Aquivion is not. Adding 10 wt% of sepiolite in Aquivion, be it functionnalized or not, resulted in a very significant increase of the membranes swelling, 116% and 121% respectively for Aq/SEP10 and Aq/SEP-F10. The observed impact of sepiolite on swelling is consistent with the evolution of the water uptake.

As shown in Fig. 4e, an additional swelling was observed for wet membranes between room temperature and 100 °C. Again, the

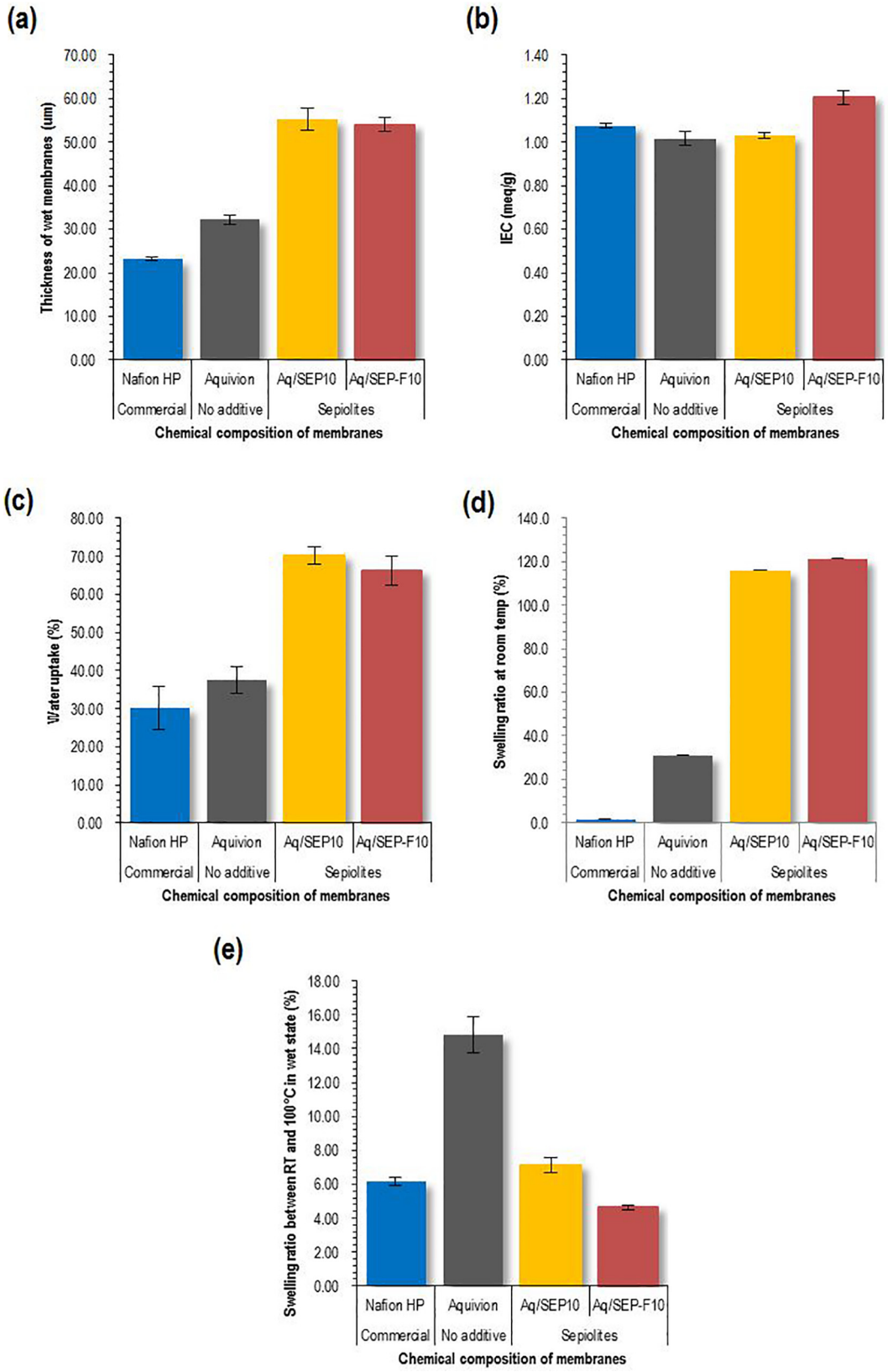

Fig. 4. Data on (a) thickness, (b) ion exchange capacity, (c) water uptake, (d) swelling between dry and wet states ar room temperature and (e) swelling in wet state between room temperature and boiling water (100 °C): commercially available Nafion HP and pristine Aquivion and Aquivion composite membranes containing 10 wt% pristine and fluorinated sepiolites.

reference membrane Nafion HP, reinforced, showed a rather low swelling (6%) compared to the prepared pristine Aquivion membrane (15%). The insertion of 10 wt% of sepiolite, regardless of the functionalization, resulted in a very significant reduction of the thickness swelling of composite membranes of about 50% compared to the pristine Aquivion membrane.

3.2.5. Homogeneity of composite membranes

Fig. 5 displays FE-SEM cross-section images of the different membranes studied. EDS analysis was performed at both the edge of the membranes as well as in the center of the cross section in order to follow the chemical composition through the membranes and to get insights on the nanoclay repartition. Silicon, representative of sepiolite, and fluorine, mainly representative of Aquivion, were specifically analyzed. Their atomic ratio (Si/F) was then considered as an indicator for homogeneity. A constant value of Si/F suggests that the nanoclay can be considered as homogeneously distributed though the membrane. Otherwise, nanoclay agglomeration and sedimentation process during the membrane preparation, can be suspected.

The addition of pristine sepiolite resulted in rather inhomogeneous composite membrane (Aq/SEP10). The large difference in Si/F values analyzed through the membrane is consistent with the presence of large agglomerates observed on Fig. 5d.

Fluorination seems to improve the homogeneity of the composite membrane. Less agglomerates are observed in the cross section of Aq/SEP-F10 (Fig. 3g) and the difference in Si/F ratios is also smaller, see Fig. 6. Functionalization was expected to improve the compatibility between sepiolite and Aquivion. The perfluorinated groups (i.e., $-C_7F_{15}$) of the N-(3-triethoxysilylpropyl)-perfluorooctanoamide grafting agent should indeed lead to good fluorine-fluorine interactions with the hydrophobic domains of Aquivion, resulting in improved compatibility and homogeneity [35]. However the repartition of nanoclays can be improved further.

3.2.6. Dynamic mechanical analysis (DMA)

The mechanical strength of the membranes can be analyzed by DMA (Fig. 7). It is clear from Fig. 7 that Aquivion is more mechanically stable at intermediate temperatures than Nafion HP. The drop of G' arose indeed at a much higher temperature for Aquivion, showing a larger glassy domain. The Aquivion membrane exhibited a higher glass transition temperature (T_g) that stands at 140 °C.

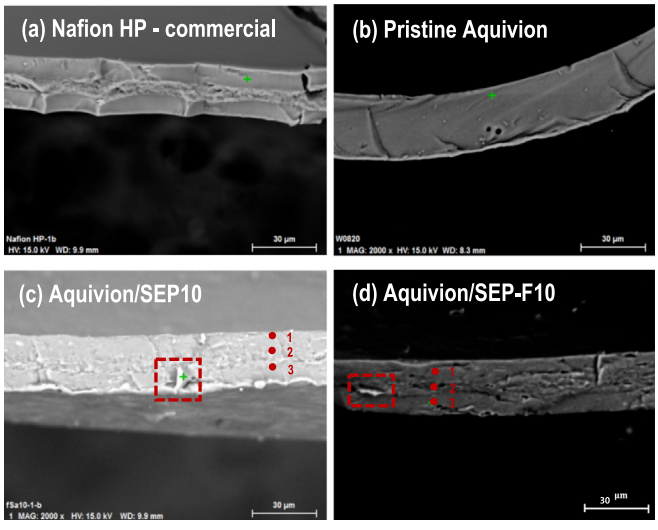

Fig. 5. FE-SEM images on (a) commercially available Nafion HP, (b) pristine Aquivion, and (c) Aq/SEP10 and (d) Aq/SEP-F10 membranes.

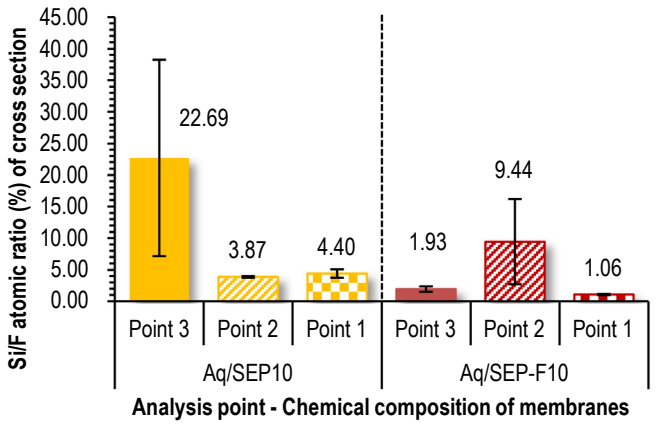

Fig. 6. Si/F atomic ratio (%) analyzed using EDS performed on sepiolite-based membranes: Aq/SEP10 vs. Aq/SEP-F10.

The addition of 10 wt% sepiolite in Aquivion (Aq/SEP-10) resulted in improved performance. The stiffness of the composite membrane at intermediate temperature is similar to that of pure Aquivion membrane and Nafion HP. The glassy domain is however larger and the T_g is shifted to 170 °C.

The fluorination of sepiolite resulted in a higher stiffness (higher G' value). The T_g of the prepared composite membrane (Aq/SEP-F10) seems to be higher than 170 °C.

These results indicate that the added sepiolite acts as a reinforcement, all the more so that it is fluorinated, and that the compatibility with Aquivion is improved through fluorination.

3.2.7. Chemical stability

As above-mentioned in introduction section, sepiolite may contain some iron ions which could participate to the membrane degradation in the presence of hydrogen peroxide. For this reason, it was verified whether composite membranes containing sepiolite are chemically stable or not in the conditions of a modified Fenton test, according to the analytical method explained in section 2.3.9. The membrane sample is immersed in a mixture of H_2O_2 and H_2SO_4, the hypothesized source of Fe^{2+} being the sepiolite. The concentration of fluorine ions from the degradation reactions is followed with a specific electrode. The influence of the fluorination was studied.

The iron content in sepiolite was analyzed with EDS during SEM observation and related to that of silicon. Fe/Si atomic ratio measured in pure and fluorinated sepiolite nanoparticles amounted to 0.65% ± 0.09% and 0.76% ± 0.10%, respectively. This was estimated high enough to justify a chemical stability study applying the modified Fenton test described in the experimental section. Pristine Aquivion and Nafion HP do not contain iron but were also analyzed the same way as references. Results for all the membranes tested at different reaction time from 4 to 96 h are shown in Fig. 8.

The evolution of the fluoride (F^-) concentration with time is similar for all the membranes tested: the longer the treatment the higher the F^- concentration. The F^- concentration is significantly higher for the Aquivion membrane than for the reference Nafion HP membrane, approximately double. However, the F^- concentration is rather limited even after 96 h of treatment since it is always quite close to that measured for the blank solution (red dotted line on Fig. 8).

It is noticeable that the presence of sepiolite does not amplify the membrane degradation. The fluoride concentration measured for composite membranes is even smaller, halved after 96 h, compared to that measured for the reference membrane Nafion HP.

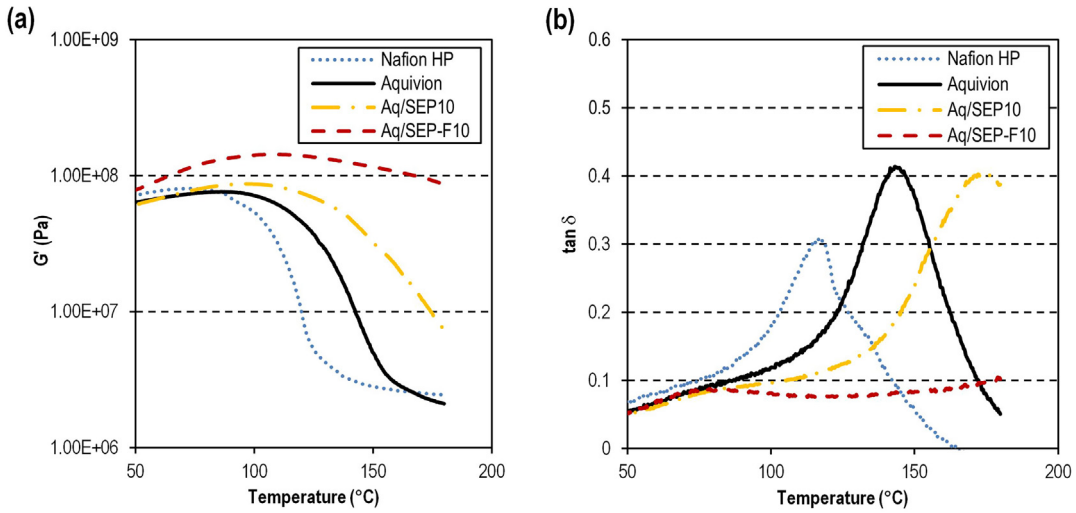

Fig. 7. Data on DMA - (a) G′ and (b) tan delta - of Nafion HP, pristine Aquivion, and Aquivion composite membranes blended with pristine sepiolite or fluorinated sepiolite.

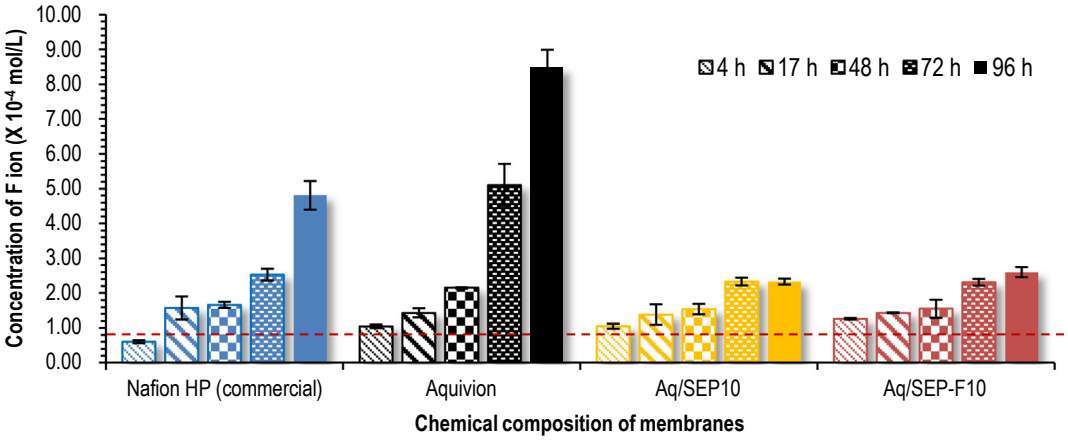

Fig. 8. Fluoride (F^-) concentration analyzed after immersion in H_2O_2/H_2SO_4 for Nafion HP, pristine Aquivion, Aq/SEP and Aq/SEP-F membranes. Red dotted line represents the fluorine concentration of 4.4 M H_2O_2/1.25 mM H_2SO_4 solution (blank test): $0.82 \times 10^{-4} \pm 0.08 \times 10^{-4}$ mol/L.

No significant difference was observed among the various composite membranes. The fluorination of sepiolite has no impact on the degradation of the composite membranes. It can be concluded that the fluorination is not detrimental to the membrane chemical stability. Moreover, a comparison between the two reference membranes (i.e., pristine Aquivion and Nafion HP) and the composite membranes indicates that the presence of sepiolite in the composite membranes does not result in the formation of radicals (i.e., HO· and HO_2·) which may attack the C-F bonds.

Rio's group reported that sepiolite does not contain any Fe^{2+} ions, based on the analysis of twenty kinds of different sepiolites from various provenances such as Madrid, Toledo, Zaragoza, California and so on [56]. This is consistent with our observation. Sepiolite (Tolsa company) used for the membrane preparation in this study is mined at Madrid, Spain. The fact that no degradation was observed showed that the Fe^{3+} ions from sepiolite are not reduced to Fe^{2+}. It should be noted that the iron ion can circulate between Fe^{2+} and Fe^{3+} when free radicals are present [57,58].

3.2.8. Proton conductivity

A fuel cell membrane requires high proton conductivity originated from the mobility of ion carriers. The proton transfer phenomena in ionomeric polymer matrices are classified into Grotthuss and vehicular mechanisms, which were already described in section 3.2.4. In the study, the through-plane resistance of prepared membranes was measured using AC impedance spectroscopy under conditions of different temperature (50°C, 70°C, and 90°C) and relative humidity (25%, 50%, 75%, and 90%). The proton conductivity is then calculated from the measured resistance taking the membrane thickness into account (see section 3.2.1). It was not possible to measure the thickness during the resistance measurement. Since the membrane was hydrated in the measurement cell we chose to consider the thickness measured in wet conditions to calculate the proton conductivities. The real conductivities may vary from the calculated ones. Nevertheless, it is noteworthy that the conductivities calculated here for Aquivion at 90 °C and 25 %RH or 90 %RH are close to values reported in literature (cf. Fig. 9).

As a general rule the higher the temperature and/or the relative humidity, the higher the proton conductivity (i.e., the lower the resistance). As expected, the impact of the relative humidity is much more pronounced than that of the temperature.

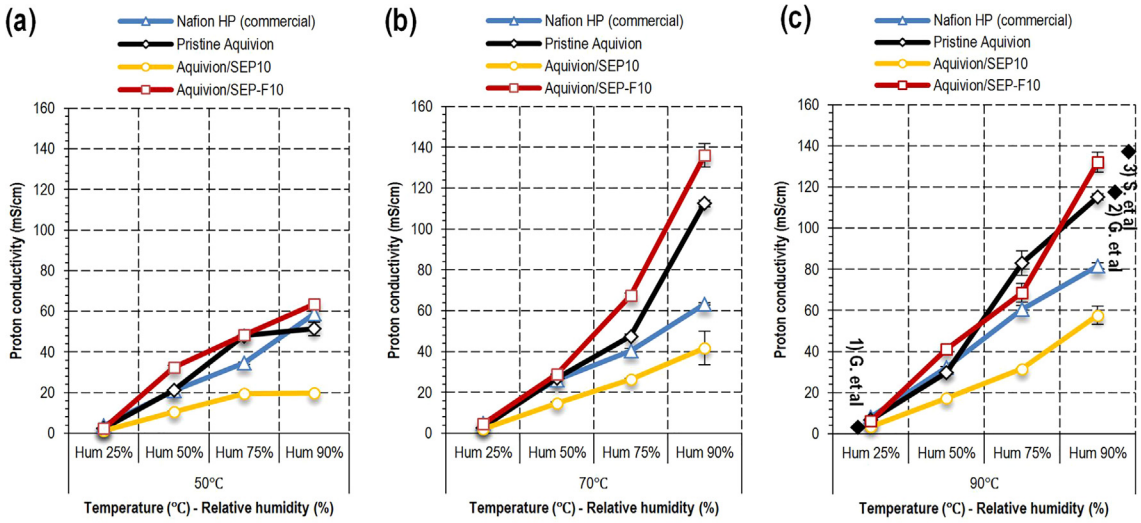

1) Gebert et al, 10 mS/cm at 95°C , 25% RH (Aquivion E79-03S) [59].
2) Giancola et al, 118 mS/cm at 80°C, 95% RH (Aquivion EW 830 g/eq) [61]
3) Skulimowska et al, 138 mS/cm at 90°C, 95% RH (Aquivion E87-12S) [60]

Fig. 9. Influence of temperature and relative humidity on proton conductivity for various PEMs: Nafion HP, pristine Aquivion, Aquivion/SEP10 and Aquivion/SEP-F10 membranes. 1) Gebert et al., 10 mS/cm at 95°C , 25% RH (Aquivion E79-03S) [59]. 2) Giancola et al., 118 mS/cm at 80°C, 95% RH (Aquivion EW 830 g/eq) [61] 3) Skulimowska et al., 138 mS/cm at 90°C, 95% RH (Aquivion E87-12S) [60].

As shown in Fig. 9, pristine Aquivion membrane generally showed a better conductivity than Nafion HP. It is well known that Aquivion has improved properties compared with Nafion series due to shorter side-chains, larger crystallinity, higher glass transition temperature and lower equivalent weight [5,6].

The proton conductivity of the pristine Aquivion membrane obtained in this study was very similar to that found in the literature at similar conditions [59,60]. It reached approximately 115 mS/cm at 90 °C and 90% RH.

Blending of pristine sepiolite (i.e., SEP10) with Aquivion resulted in a decrease of the proton conductivity compared with pristine Aquivion membrane and Nafion HP. This may be related to the observed agglomeration of sepiolite and possible blocking of the ionic path thus hindering the movement of protons within the composite membranes.

The fluorination of sepiolite (i.e., SEP-F10) enhanced the conductivity of the composite membrane to a value that was close or even slightly higher, depending on the conditions, to that of pristine Aquivion. This may be due to the improved affinity of the functionalized nanoclay with the ionomer, as already described in section 3.2.2, or to a better ionomer chain organization during membrane formation.

However, whatever the temperature, between 25 °C and 90 °C, the introduction of sepiolite in Aquivion does not seem to improve the conductivity at low relative humidity.

3.2.9. Fuel cell performance

In wet conditions the initial polarization curves are rather similar (see Fig. 10a). The mass transport limitation occurs at lower cell voltages for the Aquivion and composite membranes. This may be due to the presence of sepiolite for the latter.

In all other dryer conditions (dry, low pressure and HAST conditions) the performances of the composite membranes are slightly better before 0.8 A/cm^2, especially when the sepiolite is fluorinated (see Fig. 8b–d). The presence of sepiolite in the composite membranes is thus beneficial in dry conditions. In so-called "dry conditions" (see Fig. 10b) the mass transport limitations looks however much more pronounced than in wet conditions (see Fig. 8a).

The HAST cycles proved very severe on all MEAs, all tests were interrupted after less than 15 h. The tests all finished in the same way, with a drastic increase in crossover currents, short resistances lower than 1 Ω cm^2 and a significant decrease in OCV and fuel cell performances.

At 0.6 A/cm^2, the cell voltage of the MEA incorporating Aquivion based membranes, pristine or composite, is, until 10 h of cycling, systematically higher than that of the Nafion® HP based MEA (see Fig. 11a). The decrease in performance with time after HAST cycles is comparable for all the tested membranes except pristine Aquivion. After 10 h of cycling, the performance of the pristine Aquivion based MEA dropped significantly. It is noteworthy that the incorporation of sepiolite in Aquivion resulted in a limited decrease of performance. The presence of sepiolite does not however significantly impact the durability of the MEA in the tested conditions.

The initial hydrogen crossover of the composite membranes is slightly higher than that of the pristine Aquivion membrane or Nafion® HP (see Fig. 11b). This impacted the open circuit voltage (OCV) which was slightly lower for composites membranes compared to that of pristine Aquivion based MEAs (see Fig. 10d). Surprisingly, if the fluorination of sepiolite did impact the initial hydrogen crossover, the effect on the OCV is rather limited. The hydrogen crossover increased with time during HAST tests for all membranes tested and only that of Nafion® HP could be measured after 10 h of cycling. From the results obtained after 5 h of cycling it looks clear that the hydrogen cross over is much more limited for sepiolite based composite membranes compared to the pristine Aquivion membrane. So even if the level of hydrogen crossover was still higher than that obtained with Nafion® HP, it came out that the presence of sepiolite, modified or not, may thus be beneficial in the case of Aquivion based composite membranes. However the fluorination of sepiolite did not reduce the hydrogen crossover even if improved compatibility with Aquivion was expected. Further

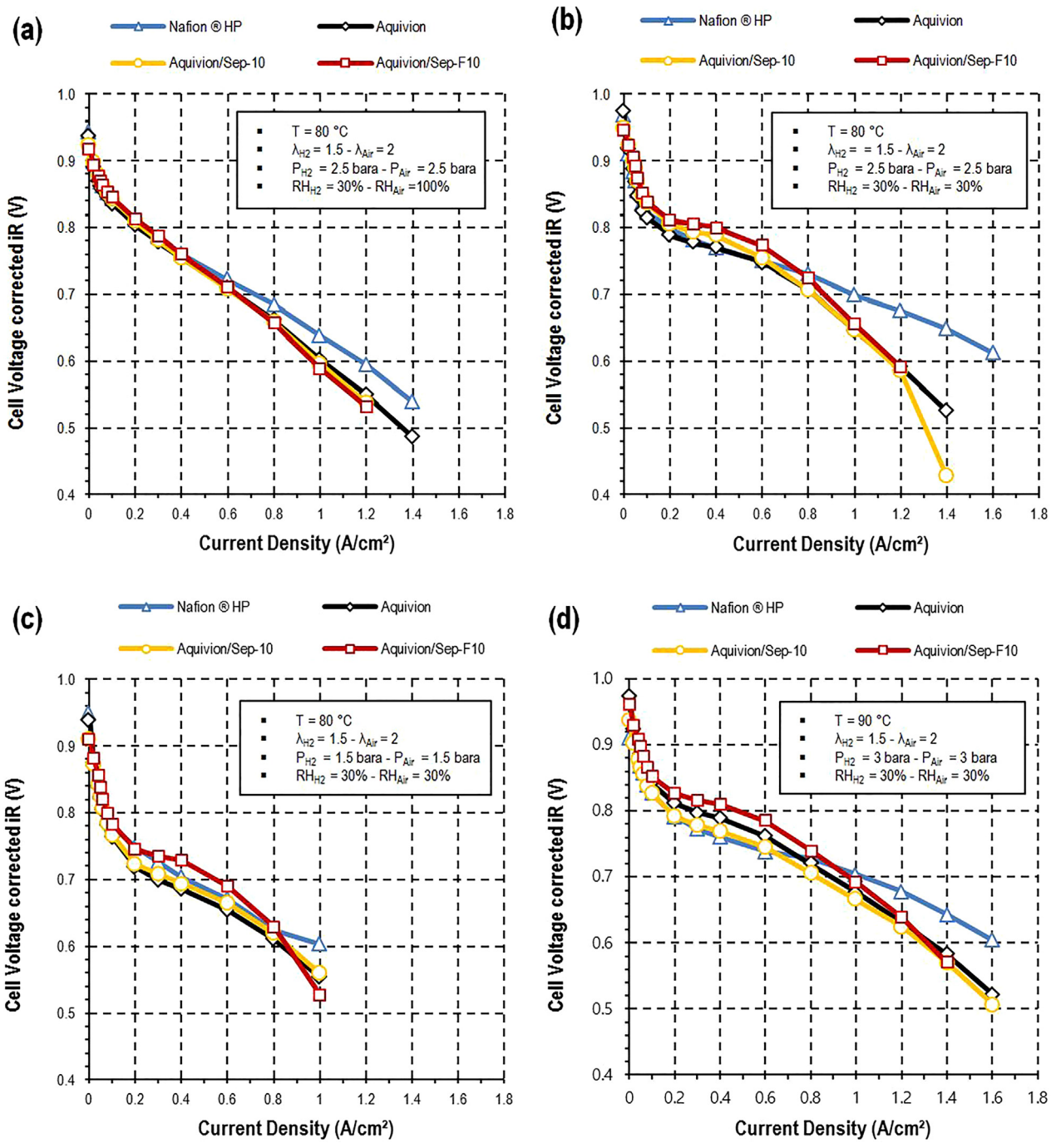

Fig. 10. Polarization curves of membrane electrode assemblies (MEAs) based on Nafion HP and different Aquivion membranes: (a) wet, (b) dry, (c) low pressure and (d) HAST initial conditions.

minimizing the hydrogen crossover is a promising route for improvement that should result in much better performances.

4. Conclusions

Sepiolite was successfully grafted with fluorinated group. Aquivion composite membranes were prepared by blending with sepiolite (i.e., SEP) or fluorine grafted sepiolite (i.e., SEP-F), and they were compared with commercially available Nafion HP and pristine Aquivion. A number of conclusions related to physicochemical properties of composite membranes can be drawn:

- The incorporation of pristine sepiolite into the Aquivion matrix led to larger water uptake (+85%) and swelling (+73% between dry and wet states at room temperature) and better mechanical properties (Tg shifted to 170 °C from 140 °C). The resulting composite membrane displayed similar IEC and chemical stability, but showed reduced dispersion of fillers and proton conductivity, the composite membranes being thicker after water absorption than pristine Aquivion and Nafion HP.
- The fluorination of sepiolite proved to be beneficial. It resulted in better dispersion state of the additive inside the polymer phase of the composite membrane. The mechanical strength,

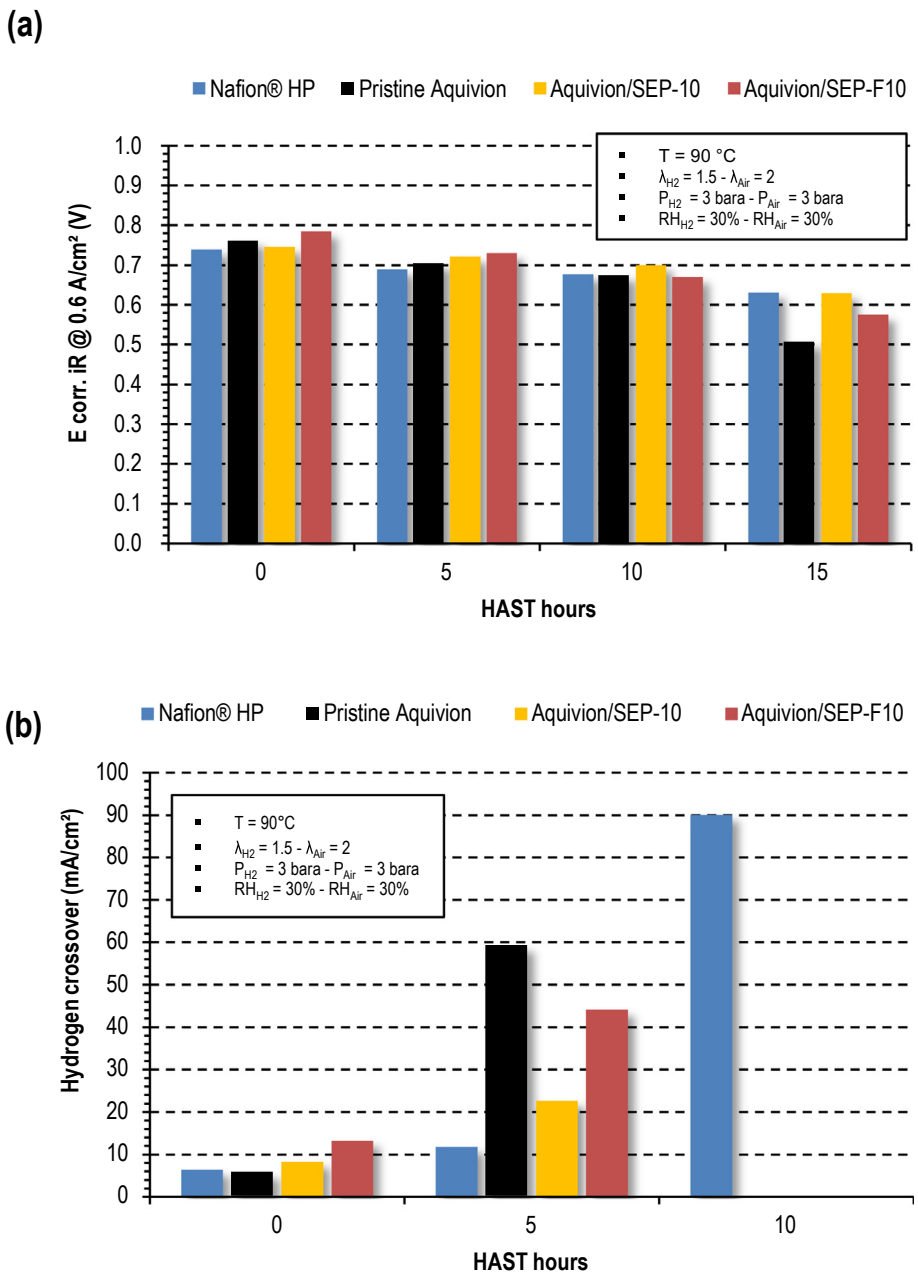

Fig. 11. Evolution of (a) the voltage at 0.6 A/cm^2 and (b) the hydrogen crossover for the different MEAs during the HAST.

chemical stability, as well as the proton conductivity were slightly improved, without impacting the water uptake, the thickness nor the IEC.

- Electrolyte membranes were incorporated in MEAs to be tested in single cell. Slightly better performances were achieved with composites membranes compared to Nafion HP or pristine Aquivion, especially at intermediate current density and low relative humidity. The best performance was obtained with the fluorinated sepiolite based composite membrane.

Further study is needed to optimize the amount of nanofiber additives inside the Aquivion phase, in order to optimize the membrane characteristics and especially reduce the hydrogen crossover. The composite membrane thicknesses also have to be reduced in order to limit the resistance loss of the MEAs.

Acknowledgements

This study was supported by funding under the COMEHTE project (contract number ANR-15-CE05-0025-01) granted from French National Research Agency (ANR). The authors wish to thank Patrick Leroux (PERSEE center), Pierre Ilbizian (PERSEE center), Cedric Sernissi (PERSEE center), Suzanne Jacomet (CEMEF center) Gabriel Monge (CEMEF center), Loïc Dumazert (C2MA center) and Benjamin Gallard (C2MA center) for technical support.

References

[1] M. Winter, R.J. Brodd, What Are Batteries, Fuel Cells, and Supercapacitors? ACS Publications, 2004.

[2] B.C. Steele, A. Heinzel, Materials for Fuel-Cell Technologies, Materials for Sustainable Energy: A Collection of Peer-Reviewed Research and Review Articles from, Nature Publishing Group, World Scientific, 2011, pp. 224–231.

[3] J.-M. Thomassin, C. Pagnoulle, D. Bizzari, G. Caldarella, A. Germain, R. Jérôme, Improvement of the barrier properties of Nafion® by fluoro-modified montmorillonite, Solid State Ionics 177 (2006) 1137–1144.
[4] K. Kreuer, On the development of proton conducting polymer membranes for hydrogen and methanol fuel cells, J. Membr. Sci. 185 (2001) 29–39.
[5] J. Li, M. Pan, H. Tang, Understanding short-side-chain perfluorinated sulfonic acid and its application for high temperature polymer electrolyte membrane fuel cells, RSC Adv. 4 (2014) 3944–3965.
[6] A. Stassi, I. Gatto, E. Passalacqua, V. Antonucci, A. Arico, L. Merlo, C. Oldani, E. Pagano, Performance comparison of long and short-side chain perfluorosulfonic membranes for high temperature polymer electrolyte membrane fuel cell operation, J. Power Sources 196 (2011) 8925–8930.
[7] A. Aricò, A. Di Blasi, G. Brunaccini, F. Sergi, G. Dispenza, L. Andaloro, M. Ferraro, V. Antonucci, P. Asher, S. Buche, High temperature operation of a solid polymer electrolyte fuel cell stack based on a new ionomer membrane, Fuel Cells 10 (2010) 1013–1023.
[8] A.-C. Dupuis, Proton exchange membranes for fuel cells operated at medium temperatures: materials and experimental techniques, Prog. Mater. Sci. 56 (2011) 289–327.
[9] A. Chandan, M. Hattenberger, A. El-Kharouf, S. Du, A. Dhir, V. Self, B.G. Pollet, A. Ingram, W. Bujalski, High temperature (HT) polymer electrolyte membrane fuel cells (PEMFC)–A review, J. Power Sources 231 (2013) 264–278.
[10] S. Peighambardoust, S. Rowshanzamir, M. Amjadi, Review of the proton exchange membranes for fuel cell applications, Int. J. Hydrogen Energy 35 (2010) 9349–9384.
[11] R. Nagarale, W. Shin, P.K. Singh, Progress in ionic organic-inorganic composite membranes for fuel cell applications, Polym. Chem. 1 (2010) 388–408.
[12] A.K. Mishra, S. Bose, T. Kuila, N.H. Kim, J.H. Lee, Silicate-based polymer-nanocomposite membranes for polymer electrolyte membrane fuel cells, Prog. Polym. Sci. 37 (2012) 842–869.
[13] W. Zhengbang, H. Tang, P. Mu, Self-assembly of durable Nafion/TiO2 nanowire electrolyte membranes for elevated-temperature PEM fuel cells, J. Membr. Sci. 369 (2011) 250–257.
[14] B. Matos, E. Aricó, M. Linardi, A. Ferlauto, E. Santiago, F. Fonseca, Thermal properties of Nafion–TiO2 composite electrolytes for PEM fuel cell, J. Therm. Anal. Calorim. 97 (2009) 591.
[15] V. Di Noto, R. Gliubizzi, E. Negro, G. Pace, Effect of SiO2 on relaxation phenomena and mechanism of ion conductivity of [Nafion/(SiO2) x] composite membranes, J. Phys. Chem. B 110 (2006) 24972–24986.
[16] F. Pereira, K. Vallé, P. Belleville, A. Morin, S. Lambert, C. Sanchez, Advanced mesostructured hybrid silica– nafion membranes for high-performance PEM fuel cell, Chem. Mater. 20 (2008) 1710–1718.
[17] N.H. Jalani, K. Dunn, R. Datta, Synthesis and characterization of Nafion®-MO2 (M= Zr, Si, Ti) nanocomposite membranes for higher temperature PEM fuel cells, Electrochim. Acta 51 (2005) 553–560.
[18] A. Saccà, A. Carbone, R. Pedicini, M. Marrony, R. Barrera, M. Elomaa, E. Passalacqua, Phosphotungstic acid supported on a nanopowdered ZrO2 as a filler in nafion-based membranes for polymer electrolyte fuel cells, Fuel Cells 8 (2008) 225–235.
[19] A. D'Epifanio, M.A. Navarra, F.C. Weise, B. Mecheri, J. Farrington, S. Licoccia, S. Greenbaum, Composite nafion/sulfated zirconia membranes: effect of the filler surface properties on proton transport characteristics, Chem. Mater. 22 (2009) 813–821.
[20] Y. Zhai, H. Zhang, J. Hu, B. Yi, Preparation and characterization of sulfated zirconia (SO42−/ZrO2)/Nafion composite membranes for PEMFC operation at high temperature/low humidity, J. Membr. Sci. 280 (2006) 148–155.
[21] D.J. Kim, M.J. Jo, S.Y. Nam, A review of polymer–nanocomposite electrolyte membranes for fuel cell application, J. Ind. Eng. Chem. 21 (2015) 36–52.
[22] P. Kongkachuichay, S. Pimprom, Nafion/Analcime and Nafion/Faujasite composite membranes for polymer electrolyte membrane fuel cells, Chem. Eng. Res. Des. 88 (2010) 496–500.
[23] E. Şengül, H. Erdener, R.G. Akay, H. Yücel, N. Bac, İ. Eroğlu, Effects of sulfonated polyether-etherketone (SPEEK) and composite membranes on the proton exchange membrane fuel cell (PEMFC) performance, Int. J. Hydrogen Energy 34 (2009) 4645–4652.
[24] B.P. Tripathi, M. Kumar, V.K. Shahi, Highly stable proton conducting nanocomposite polymer electrolyte membrane (PEM) prepared by pore modifications: an extremely low methanol permeable PEM, J. Membr. Sci. 327 (2009) 145–154.
[25] A. Carbone, A. Saccà, I. Gatto, R. Pedicini, E. Passalacqua, Investigation on composite S-PEEK/H-BETA MEAs for medium temperature PEFC, Int. J. Hydrogen Energy 33 (2008) 3153–3158.
[26] A. Filippov, D. Khanukaeva, D. Afonin, G. Skorikova, E. Ivanov, V. Vinokurov, Y. Lvov, Transport properties of novel hybrid cation-exchange membranes on the base of MF-4SC and halloysite nanotubes, J. Mater. Sci. Chem. Eng. 3 (2015) 58.
[27] G. Cavallaro, R. De Lisi, G. Lazzara, S. Milioto, Polyethylene glycol/clay nanotubes composites, J. Therm. Anal. Calorim. 112 (2013) 383–389.
[28] M. Oroujzadeh, S. Mehdipour-Ataei, M. Esfandeh, Microphase separated sepiolite-based nanocomposite blends of fully sulfonated poly (ether ketone)/non-sulfonated poly (ether sulfone) as proton exchange membranes from dual electrospun mats, RSC Adv. 5 (2015) 72075–72083.
[29] F.J. Fernandez-Carretero, K. Suarez, O. Solorza, E. Riande, V. Compan, PEMFC performance of MEAs based on Nafion® and sPSEBS hybrid membranes, J. New Mater. Electrochem. Syst. 13 (2010) 191–199.
[30] P. Bébin, M. Caravanier, H. Galiano, Nafion®/clay-SO3H membrane for proton exchange membrane fuel cell application, J. Membr. Sci. 278 (2006) 35–42.
[31] J.-H. Chang, J.H. Park, G.-G. Park, C.-S. Kim, O.O. Park, Proton-conducting composite membranes derived from sulfonated hydrocarbon and inorganic materials, J. Power Sources 124 (2003) 18–25.
[32] I. Nicotera, A. Enotiadis, K. Angjeli, L. Coppola, D. Gournis, Evaluation of smectite clays as nanofillers for the synthesis of nanocomposite polymer electrolytes for fuel cell applications, Int. J. Hydrogen Energy 37 (2012) 6236–6245.
[33] F. Mura, R. Silva, A. Pozio, Study on the conductivity of recast Nafion®/montmorillonite and Nafion®/TiO2 composite membranes, Electrochim. Acta 52 (2007) 5824–5828.
[34] K. Fatyeyeva, J. Bigarré, B. Blondel, H. Galiano, D. Gaud, M. Lecardeur, F. Poncin-Epaillard, Grafting of p-styrene sulfonate and 1, 3-propane sultone onto Laponite for proton exchange membrane fuel cell application, J. Membr. Sci. 366 (2011) 33–42.
[35] C. Beauger, G. Lainé, A. Burr, A. Taguet, B. Otazaghine, Improvement of Nafion®-sepiolite composite membranes for PEMFC with sulfo-fluorinated sepiolite, J. Membr. Sci. 495 (2015) 392–403.
[36] C. Beauger, G. Lainé, A. Burr, A. Taguet, B. Otazaghine, A. Rigacci, Nafion®–sepiolite composite membranes for improved proton exchange membrane fuel cell performance, J. Membr. Sci. 430 (2013) 167–179.
[37] H. Zhang, T. Zhang, J. Wang, F. Pei, Y. He, J. Liu, Enhanced proton conductivity of sulfonated poly (ether ether ketone) membrane embedded by dopamine-modified nanotubes for proton exchange membrane fuel cell, Fuel Cells 13 (2013) 1155–1165.
[38] A.K. Mishra, T. Kuila, N.H. Kim, J.H. Lee, Effect of peptizer on the properties of Nafion–Laponite clay nanocomposite membranes for polymer electrolyte membrane fuel cells, J. Membr. Sci. 389 (2012) 316–323.
[39] X. Liu, S. He, G. Song, H. Jia, Z. Shi, S. Liu, L. Zhang, J. Lin, S. Nazarenko, Proton conductivity improvement of sulfonated poly (ether ether ketone) nanocomposite membranes with sulfonated halloysite nanotubes prepared via dopamine-initiated atom transfer radical polymerization, J. Membr. Sci. 504 (2016) 206–219.
[40] M.-K. Song, S.-B. Park, Y.-T. Kim, K.-H. Kim, S.-K. Min, H.-W. Rhee, Characterization of polymer-layered silicate nanocomposite membranes for direct methanol fuel cells, Electrochim. Acta 50 (2004) 639–643.
[41] J.-M. Thomassin, C. Pagnoulle, G. Caldarella, A. Germain, R. Jérôme, Contribution of nanoclays to the barrier properties of a model proton exchange membrane for fuel cell application, J. Membr. Sci. 270 (2006) 50–56.
[42] A. Rico-Zavala, F.V. Matera, N. Arjona, J. Rodríguez-Morales, J. Ledesma-Garcia, M. Gurrola, L. Arriaga, Nanocomposite membrane based on SPEEK as a perspectives application in electrochemical hydrogen compressor, Int. J. Hydrogen Energy 44 (2019) 4839–4850.
[43] C. Felice, S. Ye, D. Qu, Nafion– montmorillonite nanocomposite membrane for the effective reduction of fuel crossover, Ind. Eng. Chem. Res. 49 (2010) 1514–1519.
[44] R. Kamble, M. Ghag, S. Gaikawad, B.K. Panda, Halloysite nanotubes and applications: a review, J. Adv. Sci. Res. 3 (2012).
[45] H. Zhang, Y. He, J. Zhang, L. Ma, Y. Li, J. Wang, Constructing dual-interfacial proton-conducting pathways in nanofibrous composite membrane for efficient proton transfer, J. Membr. Sci. 505 (2016) 108–118.
[46] H. Zhang, C. Ma, J. Wang, X. Wang, H. Bai, J. Liu, Enhancement of proton conductivity of polymer electrolyte membrane enabled by sulfonated nanotubes, Int. J. Hydrogen Energy 39 (2014) 974–986.
[47] F. Fernandez-Carretero, V. Compan, E. Riande, Hybrid ion-exchange membranes for fuel cells and separation processes, J. Power Sources 173 (2007) 68–76.
[48] S.H. Woo, A. Rigacci, C. Beauger, Influence of sepiolite and halloysite nanoclay additives on the water uptake and swelling of nafion based composite membranes for PEMFC: impact of the blending time on composite homogeneity, Chem. Lett. 48 (2019) 418–421.
[49] J. Qiao, M. Saito, K. Hayamizu, T. Okada, Degradation of perfluorinated ionomer membranes for PEM fuel cells during processing with H2O2, J. Electrochem. Soc. 153 (2006) A967–A974.
[50] Q. Guo, P.N. Pintauro, H. Tang, S. O'Connor, Sulfonated and crosslinked polyphosphazene-based proton-exchange membranes, J. Membr. Sci. 154 (1999) 175–181.
[51] F.N. Büchi, B. Gupta, O. Haas, G.G. Scherer, Study of radiation-grafted FEP-G-polystyrene membranes as polymer electrolytes in fuel cells, Electrochim. Acta 40 (1995) 345–353.
[52] J. Xie, D.L. Wood, D.M. Wayne, T.A. Zawodzinski, P. Atanassov, R.L. Borup, Durability of PEFCs at high humidity conditions, J. Electrochem. Soc. 152 (2005) A104–A113.
[53] C. Zhao, H. Lin, K. Shao, X. Li, H. Ni, Z. Wang, H. Na, Block sulfonated poly (ether ether ketone) s (SPEEK) ionomers with high ion-exchange capacities for proton exchange membranes, J. Power Sources 162 (2006) 1003–1009.
[54] N. Agmon, The grotthuss mechanism, Chem. Phys. Lett. 244 (1995) 456–462.
[55] K.D. Kreuer, A. Rabenau, W. Weppner, Vehicle mechanism, a new model for the interpretation of the conductivity of fast proton conductors, Angew. Chem. Int. Ed. 21 (1982) 208–209.
[56] M.S. del Río, E. García-Romero, M. Suárez, I. da Silva, L. Fuentes-Montero, G. Martínez-Criado, Variability in sepiolite: diffraction studies, Am. Mineral. 96 (2011) 1443–1454.
[57] K. Chemizmu, R. Fentona, Fenton reaction-controversy concerning the

chemistry, Ecol. Chem. Eng. 16 (2009) 347–358.
[58] W. Barb, J. Baxendale, P. George, K. Hargrave, Reactions of ferrous and ferric ions with hydrogen peroxide. Part I.—the ferrous ion reaction, Trans. Faraday Soc. 47 (1951) 462–500.
[59] M. Gebert, A. Ghielmi, L. Merlo, M. Corasaniti, V. Arcella, AQUIVION {trade mark, serif}–the short-side-chain and low-EW PFSA for next-generation PEFCs expands production and utilization, ECS Trans. 26 (2010) 279–283.
[60] A. Skulimowska, M. Dupont, M. Zaton, S. Sunde, L. Merlo, D.J. Jones, J. Rozière, Proton exchange membrane water electrolysis with short-side-chain Aquivion® membrane and IrO2 anode catalyst, Int. J. Hydrogen Energy 39 (2014) 6307–6316.
[61] S. Giancola, M. Zatoń, A. Reyes-Carmona, M. Dupont, A. Donnadio, S. Cavaliere, J. Rozière, D.J. Jones, Composite short side chain PFSA membranes for PEM water electrolysis, J. Membr. Sci. 570 (2019) 69–76.